Electronic Supplementary Material (ESI) for Physical Chemistry Chemical Physics.

Supporting Information

Direct Observation of Stepwise Intermolecular Proton and Hydrogen Transfers between Alcohols and Triplet State of 4-Nitro-1-Naphthol

Fengjin Zhang,[a] Di Zhang,[a] Yong Du,[b] Peipei Jin,[a] Yanying Zhao,[a] Xuming Zheng,[a] Jiadan Xue[a]*

Email: jenniexue@zstu.edu.cn

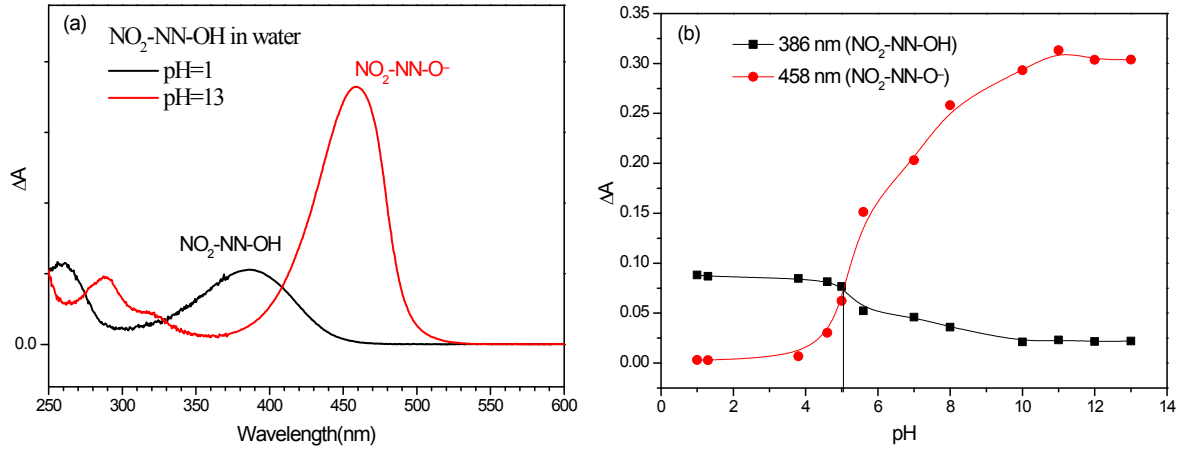

Figure 1S. UV-vis spectra (a) of NO_2-NN-OH in (black) acidic water and (red) basic water solutions, and (b) NO_2-NN-OH ground state was measured to have a pK_a=5.1

Table 1S. Pseudo first order decay or/and growth time constants fitted with exponential functions at wavelengths of 373,450 and 630 nm in ACN/EtOH mixed solutions containing various proportion of EtOH.

%[a]	t_{373}		t_{450}			t_{630}	
	***g* (ns)**	***d* (μs)**	**d_1(ns)**	***g* (ns)**	**d_2 (μs)**	**d_1(ns)**	**d_2 (μs)**
5	712(2)	42.1(0.2)	750(5)		69.4(0.3)	787(4)	43.9(0.8)
8.5	238(2)	11.7(0.3)	253(2)	10800(124)	34.2(0.3)	275(0.8)	10.3(0.2)
10	141(1)	7.7(0.01)	167(2)	7623(33)	26.9(0.2)	187(5)	10.4(0.1)
13	76(3)	4.0(0.02)	90(7)	4000(56)	20.0(0.3)	90(8)	4.8(0.2)
15	33(0.8)	2.9(0.02)		3296(85)	13.0(0.2)	57(1)	3.7(0.1)
20		1.3(0.01)		1412(100)	9.7(0.04)		1.4(0.05)
30		505[c](6)		512(4)	4.4(0.02)		
45		191[c](1)		197(2)	2.9(0.01)		
60		107[c](0.9)		108(1)	2.5(0.1)		
80		66[c](1)		66(2)	2.4(0.01)		

[a]Volume proportion and ignore the volume change after mixture of ACN and EtOH. [b]g=growth, d=decay. [c]unit:ns, [d]data in brackets are fitted errors.

Table 2S. Pseudo first order decay or/and growth time constants fitted with exponential functions at wavelengths of 315, 373,450 and 630 nm in ACN/IPA mixed solutions containing various proportion of IPA.

%[a]	t_{315}		t_{373}		t_{450}			t_{630}	
	g (ns)	***d (μs)***	***g (ns)***	***d (μs)***	***d_1(ns)***	***g (ns)***	***d_2 (μs)***	***d_1(ns)***	***d_2 (μs)***
5	874(15)	58.7(0.5)	951(3)	55.0(0.6)	1342(5)			1119(5)	49.8(1.9)
8.5	495(4)	22.9(0.1)	497(2)	22.9(0.1)	534(2)			600(4)	26.8(0.6)
10	360(13)	21.4(0.2)	382(2)	17.2(0.1)	415(5)		50.2(0.3)	478(3)	24.4(0.4)
13	191(5)	10.7(0.1)	202(1)	8.3(0.01)	209(1)		32.7(0.1)	240(1)	8.5(0.1)
15	136(2)	7.1(0.02)	139(2)	6.0(0.01)	162(2)		16.4(0.2)	164(0.4)	6.6(0.07)
20	42(0.8)	4.0(0.02)	52(0.8)	2.9(0.02)	78(3)	3078(19)	12.8(0.08)	85(1)	4.1(0.06)
30	18(0.4)	1.4(0.01)		1.1(0.04)	24(2)	1108(8)	6.9(0.1)	33(0.7)	2.0(0.04)
45		668[c](4)		511[c](4)		499(2)	5.9(0.03)		
60		381[c](3)		324[c](3)		301(1)	3.9(0.01)		

[a]Volume proportion and ignore the volume change after mixture of ACN and IPA. [b]g=growth, d=decay. [c]unit:ns. [d]data in brackets are fitted errors.

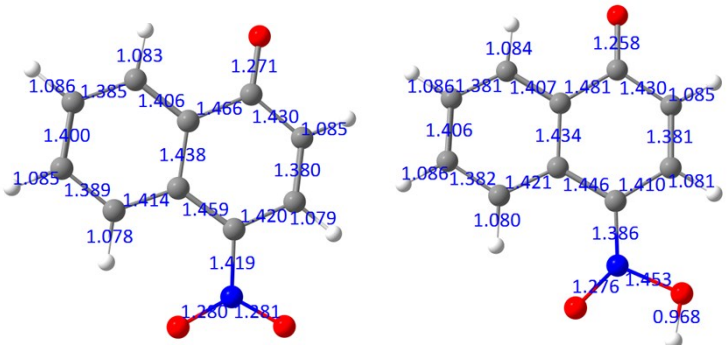

Figure 2S. Optimized structures for (left) $^3NO_2$-NN-O^- and (right) HNO_2-NN-$O^{\bullet -}$ with the DFT calculation at the level of B3LYP/6-311++G(d,p), with the bond lengths labeled nearby.

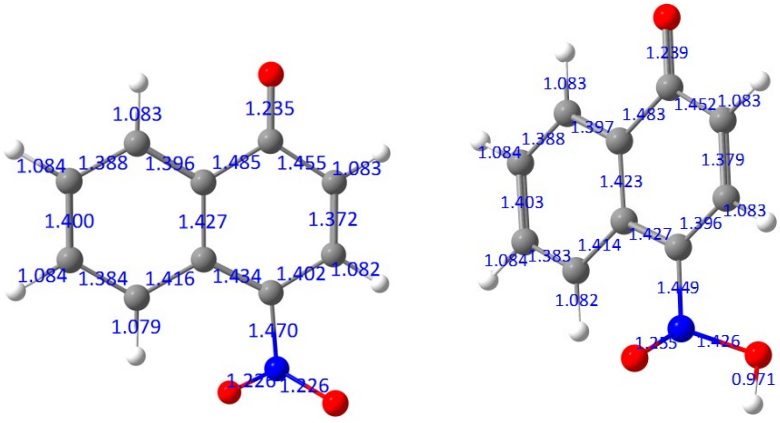

Figure 3S. Optimized structures for (left) NO_2-NN-$O^{\bullet}$ and (right) $^3HNO_2$-NN-O with the DFT calculation at the level of B3LYP/6-311++G(d,p), with the bond lengths labeled nearby.

Table 3S. DFT calculation predicted vertical transition energies (nm) and corresponding oscillator strengths for radical NO_2-NN-O$^{\bullet}$ and triplet $^3HNO_2$-NN-O at the level of B3LYP/6-311++G(d,p).

NO_2-NN-O$^{\bullet}$		$^3HNO_2$-NN-O	
transition energies (nm)	**oscillator strengths**	**transition energies (nm)**	**oscillator strengths**
596.23	0.0030	545.31	0.0031
568.16	0.0315	525.24	0.0288
481.36	0.0005	419.46	0.00520
463.20	0.0014	378.72	0.0275
406.20	**0.0430**	**343.49**	**0.0411**
399.16	**0.0370**	327.46	0.0030
350.96	0.0152	322.63	0.0048
338.80	0.0197	319.40	0.0376
326.76	0.0015	315.94	0.0303
320.62	0.0092	307.60	0.0051
309.72	0.0007	303.76	0.0024
307.58	0.0241		
303.88	0.0048		

Table 4S. Experimental transient Raman frequencies observed in single-pulse resonance Raman experiment and the DFT calculation predicted vibrational frequencies for radical HNO_2-NN-OH$^{\bullet}$

mode	Calc. Freq. (Raman activity)	Expt. Raman Shift (cm^{-1})	Descriptions
ν_{51}	1656 (19)	1642	C-C stretch
ν_{50}	1626 (20)	1624	Ring CH bend, C-C stretch, CO-H bend, NO-H bend, N=O stretch
ν_{49}	1597 (62)	1604	Ring CH bend, C-C stretch, CO-H bend, NO-H bend, N=O stretch
ν_{48}	1585(224)	1593	NO-H bend, N=O stretch, C-C stretch
ν_{47}	1553 (126)	1556	C-H bend, C-C stretch, CO-H bend, NO-H bend, N=O stretch
ν_{46}	1489 (31)		Ring CH bend, C-C stretch, CO-H bend, NO-H bend
ν_{45}	1476 (30)	1472	Ring CH bend, C-C stretch, CO-H bend, NO-H bend
ν_{44}	1432(52)	1431	Ring CH bend, C-C stretch, CO-H bend
ν_{43}	1394 (232)		C-C stretch, CO-H bend
ν_{42}	1368(90)		C-C stretch, CO-H bend, NO-H bend
ν_{41}	1320 (21)		Ring CH bend, C-C stretch, N=O stretch, NO-H bend
ν_{40}	1302 (31)	1294	N=O stretch, NO-H bend, Ring CH bend, C-C stretch

ν_{38}	1227 (23)	1219	CO-H bend, Ring CH bend, Ring C-C stretch
ν_{37}	1209 (33)		Ring CH bend
ν_{36}	1191(76)	1175	Ring CH bend, C-N stretch, Ring C-C stretch
ν_{35}	1167 (10)	1153	C-C stretch

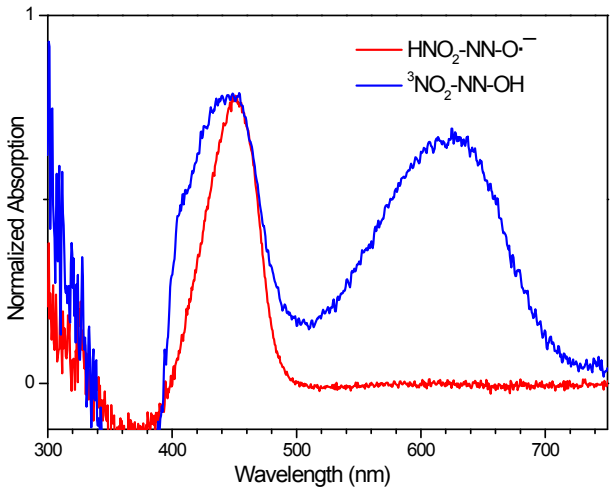

Figure 4S. Comparison of absorption spectrum of (blue) $^3NO_2$-NN-OH and (red) HNO_2-NN-$O^{\bullet -}$.

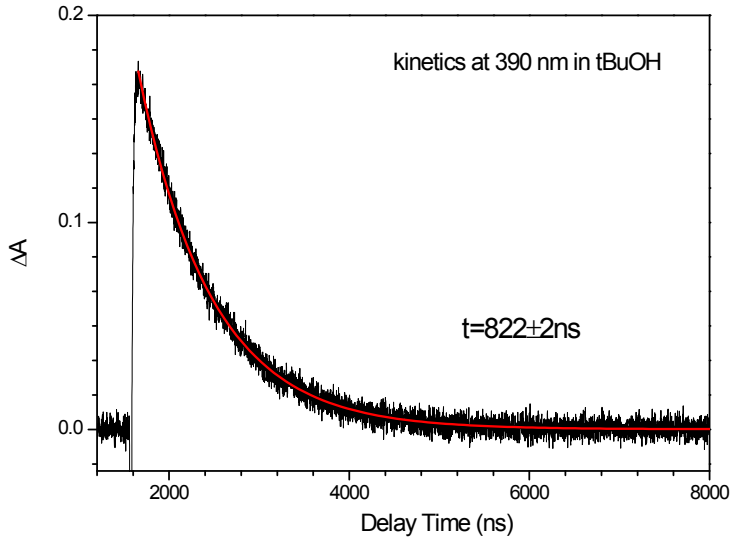

Figure 5S. Kinetics at 390 nm after 355 nm excitation of NO_2-NN-OH in neat tBuOH at 40 ℃.

Table 5S: The viscosities ($mP_a \cdot S$) of n-butanol (nBuOH) and tert-butanol (tBuOH) at some selected temperatures.

	temperature (℃)				
	20	30	40	60	80
nBuOH	2.95		1.81	1.17	
tBuOH		3.10	2.14	1.09	0.597

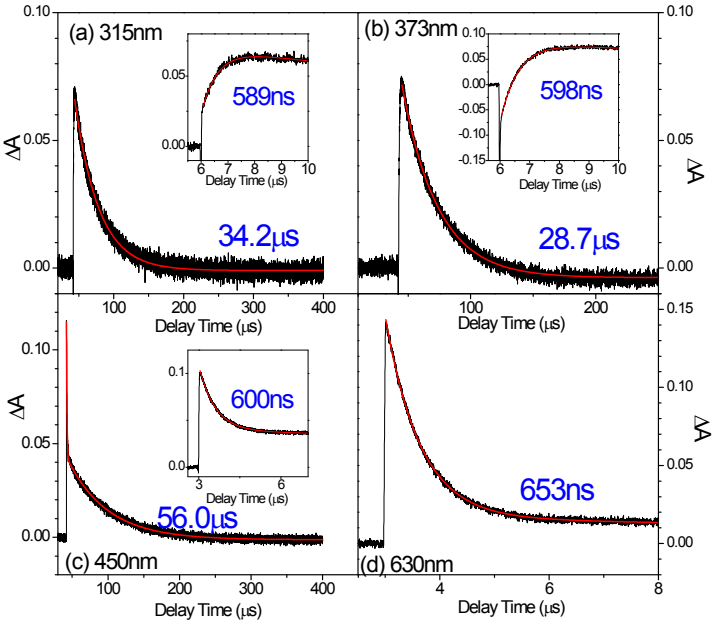

Figure 6S. Kinetic curves (black) obtained in the solution of ACN:MeOH=96:4 and exponential fitted curves (red) at (a) 315 nm, (b) 373 nm, (c) 450 nm and (d) 630 nm with fitted growth and decay time constants (blue) close to curves. The inserts are expanded window at initial time delays.

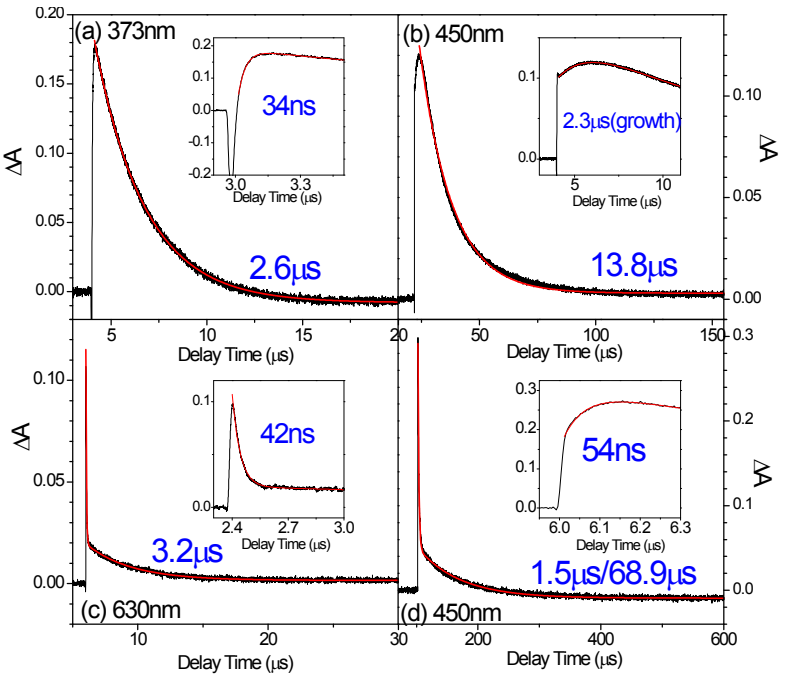

Figure 7S. Kinetic curves (black) obtained in the solution of ACN:MeOH=90:10 and exponential fitted curves (red) at (a) 373 nm, (b), 450 nm (c) 630 nm, and (d) curves in the solution of ACN:MeOH=50:50 with fitted growth and decay time constants (blue) close to curves. The inserts are expanded window at initial time delays.